

Spin-orbit interaction and spin-charge interference in resonant Raman scattering from III-V semiconductor quantum wells

V. A. Froltsov

Division of Solid State Theory, Department of Physics, Lund University, SE-223 62 Lund, Sweden

A. G. Mal'shukov

Institute of Spectroscopy, Russian Academy of Sciences, 142092 Troitsk, Moscow Region, Russia

K. A. Chao

Division of Solid State Theory, Department of Physics, Lund University, SE-223 62 Lund, Sweden

(Received 1 July 2000; revised manuscript received 30 March 2001; published 31 July 2001)

Due to the spin-orbit interaction in A_3B_5 semiconductor quantum wells, the resonant Raman scattering amplitude from the charge density excitations (CDE) interferes with that from the spin density excitations (SDE). This *spin-charge* coupling manifests itself in an asymmetry of the non-spin-flip Raman spectrum with respect to directions of circular polarizations of incident and scattered photons. Consequently, the difference spectrum obtained by subtracting the spectra taken at reversed polarizations has a band in the region of single-particle spin conserving transitions. Since CDE are involved, Coulomb screening effects are expected to have strong influence on the intensity of this band. We have calculated the difference spectrum, taking into account the long range Coulomb interaction in the random phase approximation. We have found that this interaction does not destroy the spin-charge coupling. Our calculations suggest that the experimentally observed non-spin-flip band in the Raman difference spectrum of a GaAs/AlGaAs heterostructure serves as an evidence of the CDE-SDE interference.

DOI: 10.1103/PhysRevB.64.073309

PACS number(s): 78.30.Fs, 71.70.Ej, 71.45.-d

Spin-orbit interaction (SOI) of conduction electrons in low dimensional III-V semiconductor structures are of much interest recently because of the possible spintronic applications (for a review see Ref. 1). In zinc blende semiconductors, the spin-orbit Hamiltonian derived with the $\mathbf{k} \cdot \mathbf{p}$ method has the form $\mathbf{h}(\mathbf{k}) \cdot \mathbf{s}$. At a given direction of the electron wave vector \mathbf{k} , the electron spin \mathbf{s} precesses around the vector $\mathbf{h}(\mathbf{k})$, which plays the role of an effective magnetic field. This leads to a number of experimentally observed phenomena, such as the D'yakonov-Perel' spin relaxation,² the beating patterns in Shubnikov-de Haas oscillations,³ and the specific antilocalization shape of the weak localization magnetoresistance.⁴ In addition, the spin precession, SOI also gives rise to a splitting $|\mathbf{h}(\mathbf{k})|$ of the electron conduction band which can be observed directly in electron Raman spectra. Such splitting in the low frequency electron Raman spectrum of an n -type modulation-doped GaAs/AlGaAs quantum well, observed by Jusserand *et al.*^{5,6} gives a value $|\mathbf{h}(\mathbf{k})| \simeq 0.4$ meV.

In electron Raman scattering the most detectable SOI effects appear in quantum interference phenomena which can be observed with circularly polarized photons. These effects are seen in difference spectra obtained by subtraction of Raman signals measured at reversed polarizations of both incident and scattered photons. Without SOI one would expect the difference spectra to be zero in nongyrotropic materials such as A_3B_5 semiconductors. In the presence of SOI, the intensity of difference spectra is produced by the spin-spin interference and the spin-charge interference. The spin-spin interference is due to the entanglement of light waves inelastically scattered from the spin-density fluctuations parallel and perpendicular to the quantum well interfaces. This inter-

ference gives rise to two bands of opposite signs in the difference spectrum in the region of spin-flip electronic excitations, as predicted theoretically⁷ and observed in a GaAs/AlGaAs heterostructure.⁸ The spin-spin coupling appears in both resonant and non-resonant Raman spectra.⁹ On the other hand, the spin-charge interference can be detected only under a strong resonance condition, when the incident photon energy is very close to the transition energy to one of the spin-split states.⁹ The spin-charge interference produces a third band in the difference spectrum. This band corresponds to single particle excitations in which the spin projection onto the electron momentum is conserved. The energies of SDE and CDE of this sort do not differ much, and they can be coupled to each other due to SOI. Consequently, amplitudes of light scattered inelastically from the spin and the charge fluctuations can interfere.

The difference spectrum due to the spin-charge interference was calculated in Ref. 9 where the Coulomb interaction is ignored. However, the Coulomb effects play an important role because the charge fluctuations are involved. The Coulomb interaction can screen out the single-particle CDEs, and so can shift their Raman intensity towards collective plasma modes. This screening, however, is not complete for the case of resonance Raman scattering.¹⁰ The purpose of our present work is to find out whether the Coulomb interaction can destroy completely the spin-charge interference, or some intensity can still remain in the difference spectrum. We will use the standard random phase approximation¹¹ (RPA) to treat the Coulomb screening effect. Our calculations show that under certain resonance conditions the band which remains in the difference spectrum corresponds to the spin conserving single particle transitions. In the Raman differ-

ence spectrum of a GaAs/AlGaAs heterostructure,⁸ a broad band in the region of the spin conserving single particle excitations was observed when the incident and the scattered photons have same circular polarization. This band was interpreted as an experimental artifact in the original work Ref. 8. However, assuming the same experimental conditions, our theoretical analysis on the spin-charge interference produces a band in the same frequency range where this band was observed. Therefore, our conclusion is that in the experiment Ref. 8 the spin-charge interference was observed.

We consider a degenerate electron gas in an n -doped quantum well with the growth direction along the z axis. For the assumed electron density, the Fermi energy lies in the lowest subband. The Hamiltonian of such an electron system can be divided into two parts as $\mathcal{H} = H(\mathbf{k}) + H_{so}(\mathbf{k})$, where $\mathbf{k} = (k_x, k_y)$ is a two-dimensional electron wave vector. The first part $H(\mathbf{k})$ describes the electron gas in a random δ -correlated impurity potential, and the second part is the spin-orbit interaction $H_{so}(\mathbf{k}) = \mathbf{h}(\mathbf{k}) \cdot \mathbf{s}$. The effective magnetic field $\mathbf{h}(\mathbf{k})$ contains the Dresselhaus¹² term $\mathbf{h}^D(\mathbf{k})$ and the Rashba¹³ term $\mathbf{h}^R(\mathbf{k})$.

Let $\epsilon(\mathbf{k})$ be the electron energy in the absence of spin-orbit interaction. The spin-orbit interaction splits this energy into a “+” and a “−” subband as

$$\epsilon_{\pm}(\mathbf{k}) = \epsilon(\mathbf{k}) \pm \frac{1}{2} |\mathbf{h}(\mathbf{k})|. \quad (1)$$

We will consider the low-frequency Raman scattering by the electronic transitions in the spin-split $\epsilon_{\pm}(\mathbf{k})$ subbands. We use two sets of notations $(\omega_L, \mathbf{e}_L, \mathbf{q}_L)$ and $(\omega_S, \mathbf{e}_S, \mathbf{q}_S)$ for the frequency, the polarization vector and the wave vector of the incident (subscript L) and the scattered (subscript S) electromagnetic waves, respectively. In our formulas we set $\hbar = 1$. We also define $\Omega = \omega_L - \omega_S$ as the Stokes shift, and the two-dimensional vector \mathbf{q} as the projection of the vector $\mathbf{q}_L - \mathbf{q}_S$ onto the xy plane.

In GaAs based quantum wells with sufficiently high mobility (10^5 cm²/V s or higher), the electron mean elastic scattering rate τ_e^{-1} is much less than the Stokes shift, as well as the energy separation between the $\epsilon_+(\mathbf{k})$ and $\epsilon_-(\mathbf{k})$ subbands. In this case, one can neglect the multiple scattering processes which lead to electron diffusion. Therefore after the averaging over the impurity positions with the use of the standard perturbation theory,¹⁴ the scattering cross section can be written as

$$W(\Omega, \mathbf{q}) = \sum_{m,n} W^{nm}(\Omega, \mathbf{q}),$$

$$W^{nm}(\Omega, \mathbf{q}) \propto \sum_{\mathbf{k}} \int_{-\Omega}^0 d\omega |R_{\mathbf{k}, \mathbf{k}+\mathbf{q}}^{nm}(\omega)|^2 [G_{\mathbf{k}}^{Rn}(\omega) - G_{\mathbf{k}}^{An}(\omega)]$$

$$\times [G_{\mathbf{k}+\mathbf{q}}^{Rm}(\omega + \Omega) - G_{\mathbf{k}+\mathbf{q}}^{Am}(\omega + \Omega)], \quad (2)$$

where the retarded and advanced averaged Green functions of an electron are $G_{\mathbf{k}}^{Rn}(\omega) = [G_{\mathbf{k}}^{An}(\omega)]^* = [\omega - \epsilon_n(\mathbf{k}) + i\Gamma_e]^{-1}$ and $\Gamma_e = 1/2\tau_e$.

The Raman scattering tensor $R_{\mathbf{k}, \mathbf{k}+\mathbf{q}}^{nm}$ in Eq. (2), corresponding to the transition from the state \mathbf{k} in the n th spin-split subband to the state $\mathbf{k} + \mathbf{q}$ in the m th subband, can be expressed as

$$R_{\mathbf{k}, \mathbf{k}+\mathbf{q}}^{nm}(\omega) = \gamma^{nm}(\mathbf{k}, \omega) + \sum_{i,j} T^{ij}(\mathbf{q}, \Omega) \frac{V_{\mathbf{q}}^{ijnm}}{\epsilon(\mathbf{q}, \Omega)}, \quad (3)$$

where all indices $m, n, i,$ and j take “+” or “−” for the spin-split subbands given by Eq. (1). The first term on the right-hand side represents the scattering of photon by free electrons. The second term is the first order correction of the screened Coulomb interaction. The RPA results of this correction will be analyzed later.

The first term $\gamma^{nm}(\mathbf{k}, \omega)$ corresponds to the Raman scattering by noninteracting electrons. In the case of nonresonant scattering when the detuning of the resonance is much larger than the energy separation $\Delta_{\mathbf{k}}$ between the heavy and the light hole subbands, $\gamma^{nm}(\mathbf{k}, \omega)$ was calculated in Ref. 7 and no interference was found between the Raman scattering amplitudes from SDEs and CDEs. The reason that such interference does not appear in the nonresonant case is that the contributions to $W(\Omega, \mathbf{q})$ from the “+” and the “−” states cancel each other.

For the case of strong resonance, when the detuning is much smaller than $\Delta_{\mathbf{k}}$, the scattering tensor is given by¹⁵

$$\gamma^{nm}(\mathbf{k}, \omega) = \tilde{\gamma}^{mn} G_h(\mathbf{k} - \mathbf{q}_s, \omega - \omega_S)$$

$$= \frac{\tilde{\gamma}^{mn}}{\omega - \omega_S - \epsilon_h(\mathbf{k} - \mathbf{q}_s) - i\Gamma_h}. \quad (4)$$

The resonant denominator of the hole Green function G_h allows us to tune the resonance with particular electron and hole subbands. Since holes stay deep below the Fermi level which is chosen as the zero reference energy, G_h is an advanced Green function. The hole relaxation time is $\tau_h = (2\Gamma_h)^{-1}$. Furthermore, since the valence electron energies are well below the Fermi level, the hole relaxation is determined by the inelastic electron-electron scattering and by the phonon emission, rather than by the elastic impurity scattering. Hence, it is reasonable to assume that the electron relaxation time τ_e is much longer than τ_h .

The explicit form of the tensor γ^{nm} depends strongly on which hole subband is in resonance with the incident light.⁹ Let us consider the case that the incident light is in resonance with the light hole band. For simplicity, we will ignore mixing of the heavy and the light hole subbands. Then, for scattering by the electron excitations within either the “+” or the “−” subband, we have¹⁵ $\tilde{\gamma}^{++} = \tilde{C}_0 + \tilde{\mathbf{C}}\mathbf{n}$, $\tilde{\gamma}^{--} = \tilde{C}_0 - \tilde{\mathbf{C}}\mathbf{n}$, with $\tilde{C}_0 = (P_{cv}^2/6)[\mathbf{e}_S^* \cdot \mathbf{e}_L + 3e_{S_z}^* e_{L_z}]$, $\tilde{\mathbf{C}} = -i(P_{cv}^2/6) \times [2\mathbf{P} - 3P_z \mathbf{e}_z]$. Here P_{cv} is the Kane matrix element,¹⁶ \mathbf{e}_z is a unit vector along z axis, $\mathbf{P} = \mathbf{e}_S^* \times \mathbf{e}_L$, and $\mathbf{n} = \mathbf{h}(\mathbf{k})/|\mathbf{h}(\mathbf{k})|$ is a two-dimensional unit vector.

It is easy to see that when expressed in terms of Pauli matrices, the linear combination $\tilde{\gamma}^{++} + \tilde{\gamma}^{--}$ describes the spin independent scattering by CDEs, while $\tilde{\gamma}^{++} - \tilde{\gamma}^{--}$ is associated to the z component of the spin-density fluctua-

tions. Hence, \tilde{C}_0 and \tilde{C} give, respectively, the CDEs and the SDEs scattering amplitudes. When the scattering cross section is calculated according to Eq. (2), the cross products $\tilde{C}_0\tilde{C}^*$ and $\tilde{C}_0^*\tilde{C}$ correspond to the interference of these amplitudes. As was shown in Ref. 9, due to the difference of resonance factor $G_h(\mathbf{k}-\mathbf{q}_s, \omega-\omega_s)$ at $\omega \approx \epsilon_+(\mathbf{k}_f)$ and at $\omega \approx \epsilon_-(\mathbf{k}_f)$, these terms do not cancel each other. It was also shown⁹ that this interference contribution can be detected if one takes the difference of the measured Raman peaks at $\Omega \approx \mathbf{v}_f \cdot \mathbf{q}$ for the two cases corresponding to reversing the circular polarizations of the incident and the scattered light.

In Ref. 9 the CDE-SDE interference was investigated for noninteracting electrons. However, it has been shown¹⁷ that the Coulomb interaction shifts a significant part of the Raman intensity from the single particle CDEs around $\Omega \approx \mathbf{v}_f \cdot \mathbf{q}$ to the collective plasma mode at a much higher frequency. Therefore, it is important to find out the effect of Coulomb interaction on the interference between the CDEs and the SDEs amplitudes. For the case of nonresonant Raman scattering, the intensity of the single particle CDE Raman band is dramatically decreased by the Coulomb interaction, whereas the intensity of the plasmon mode is enhanced proportionally. So there is almost no single particle CDEs amplitude left at $\Omega \approx \mathbf{v}_f \cdot \mathbf{q}$ to interfere with the SDEs at this Stokes shift. Nevertheless, it is not so for resonant Raman scattering. In this case the Coulomb interaction does not screen out the single particle CDEs, as was explained in Ref. 10. An anomalous peak due to single particle excitations is then usually observed in the resonance polarized spectra.^{6,8} Hence, it is reasonable to expect that single particle CDEs will not be screened out also in the charge-spin interference term.

The second term on the right-hand side of Eq. (3) is the first order correction due to Coulomb interaction. With respect to the eigenstate basis of the “+” and the “-” subband, the Coulomb interaction matrix elements $V_{\mathbf{q}}^{ijmn}$, which are spin independent, have the simple form $V_{\mathbf{q}}^{ijmn} = V_{\mathbf{q}} \delta_{ij} \delta_{mn}$, where $V_{\mathbf{q}}$ is the two-dimensional Fourier transform of the Coulomb potential. The RPA dielectric function has the standard form¹¹ $\epsilon_{\text{RPA}}(\mathbf{q}, \Omega) = 1 - V_{\mathbf{q}} \Pi_{\mathbf{q}, \Omega}^0$, where $\Pi_{\mathbf{q}, \Omega}^0$ is the zero-order polarization propagator. Following the standard perturbation theory approach, after averaging over impurity positions, we obtain

$$T^{ij}(\mathbf{q}, \Omega) = \sum_{\mathbf{k}} \int_{-\infty}^{+\infty} \tilde{\gamma}^{ij} G_h(\mathbf{k}-\mathbf{q}_s, \omega-\omega_s) \times G_{\mathbf{k}+\mathbf{q}}^i(\omega+\Omega) G_{\mathbf{k}}^j(\omega) \frac{d\omega}{2\pi}, \quad (5)$$

where $G_{\mathbf{k}}^i(\omega) = [\omega - \epsilon_i(\mathbf{k}) + i\Gamma_e \text{sgn}(\omega)]^{-1}$ is the averaged causal electron Green function. Making use of Eqs. (3)–(5), the cross section Eq. (2) is then expressed in terms of the electron and hole Green functions.

We introduce the difference spectrum to study the SDE-CDE interference. This spectrum is the difference of two Raman spectra taken before and after reversing the circular polarizations of both incident and scattered light. The differ-

ence spectrum consists of two parts $\Delta(W^{++} + W^{--})$ and $\Delta(W^{-+} + W^{+-})$. It is easily to see from Eqs. (2)–(5) that the first part is proportional to $\text{Re}\{\tilde{C}_0\tilde{C}^*\}$, and thus describes the spin-charge interference at $\Omega \approx \mathbf{v}_f \cdot \mathbf{q}$. Similarly, the second term is due to interference of photons inelastically scattered by in-plane component and by normal component of the SDE. The latter is proportional to $\tilde{C} \times \tilde{C}^*$, and contributes to the spin-flip bands at $\Omega \approx \mathbf{v}_f \cdot \mathbf{q} \pm |\mathbf{h}(\mathbf{k})|$.

Although these spin-spin and spin-charge interference terms contribute to different Raman bands, it is not easily to extract their respective intensities from experimentally observed spectra, because three peaks merge in a broad spectrum. Fortunately, the backscattering geometry, which is often used in Raman scattering experiments, allows to eliminate the spin-flip bands. Let us consider a typical backscattering geometry used in the experiment described in Ref. 8. The in-plane component of the scattering wave vector $\mathbf{q} = \mathbf{q}_L - \mathbf{q}_S$ is parallel to the [100] direction (x axis) and is conserved throughout the scattering process. The incident and scattered waves propagate in the xz plane. Inside the semiconductor the incident and the scattered beams make almost the same angle with the z axis, with a small difference less than 2° . In this case, as shown in Ref. 8, the vector $\tilde{C} \times \tilde{C}^*$ is very small when the polarizations of the incident and the scattered photons have equal signs. Using parameter values given in Ref. 8, it is easily to prove that $|\text{Re}\{\tilde{C}_0\tilde{C}^*\}| \gg |\tilde{C} \times \tilde{C}^*|$. Hence, the spin-charge interference dominates in the difference spectrum obtained by subtracting the Raman spectrum measured with left polarized incident and scattered photons from the Raman spectrum measured with right polarized incident and scattered photons. This is exactly the difference spectrum measured experimentally,⁸ and in the so-obtained spectrum a broad band was observed around $\Omega \approx \mathbf{v}_f \cdot \mathbf{q}$.

In our numerical calculation of the resonant difference spectrum $\Delta(W^{++} + W^{--})$, the values of the system parameters were determined according to the experimental setup and the samples used in the experiments.^{8,17} The parameter values are $q = 1.12 \times 10^5 \text{ cm}^{-1}$ for the two-dimensional wave vector, $n = 1.3 \times 10^{12} \text{ cm}^{-2}$ for the two-dimensional electron density, $\Gamma_e = 0.007 \text{ meV}$ corresponding to an electron mobility $1.19 \times 10^6 \text{ cm}^2/\text{Vs}$, and $\Gamma_h = 10\Gamma_e$. To demonstrate the essential physics we considered only linear in \mathbf{k} Dresselhaus terms of SOI. The addition of cubic terms does not change the results shown in Fig. 1 qualitatively.

Because of the integration over the angular part of the resonant denominator in Eq. (2), the single particle peak at $\Omega \approx \mathbf{v}_f \cdot \mathbf{q}$ is very sensitive to the tuning of the incident light frequency with respect to the transition energy of the spin-split subbands. This effect shows up in Fig. 1 as a drastic change of the resonant difference spectrum $\Delta(W^{++} + W^{--})$ when the resonant condition varies. The major contribution to the spectrum in Fig. 1 comes from the terms containing screened Coulomb interaction. Therefore, the Coulomb interaction enhances the SDE-CDE interference.

The collective CDEs peak in the difference spectrum can be obtained from the plasmon dispersion relation

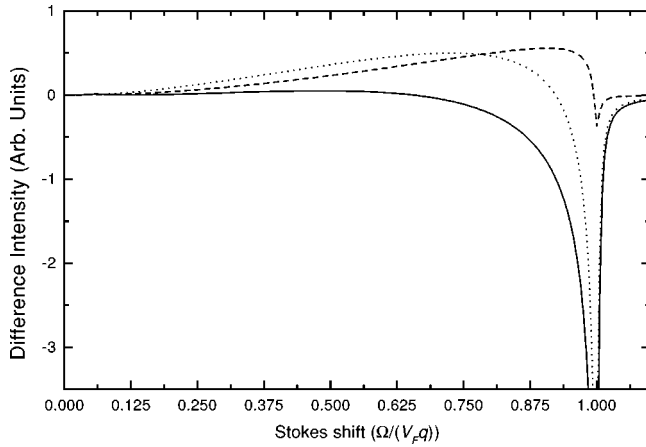


FIG. 1. Resonant difference spectrum of intraspin-split subband excitations in a 2D degenerate electron gas. Parameter values are taken as explained in the text. Different curves correspond to the resonance with the “-” spin-split subband (solid curve), with the “+” spin-split subband (dashed curve), and with the energy in the middle of “+” and “-” subbands (dotted curve).

$\text{Re}\{\varepsilon_{\text{RPA}}(\mathbf{q}, \Omega)\} = 0$. The so obtained peak at the frequency $\Omega \approx 4.25 \times v_f q$ lies far outside Fig. 1. In the difference spectrum this plasmon peak is weak compared to the single particle peak. Generally speaking, the variation of the resonance parameter, which is the denominator of the hole Green function, can change the ratio of the single particle excitation amplitude to the plasmon amplitude. However, all ampli-

tudes are reduced when the incident photon energy deviates from the resonance.

In conclusion we emphasize that the spin-orbit interaction in semiconductor quantum wells with zinc blende crystal structure leads to the coupling of CDEs and SDEs, which results in the appearance of an interference term in the Raman scattering cross section. Because of this interference, the part of the Raman spectrum, which corresponds to electron transitions within the “+” or the “-” spin-split subband, becomes asymmetric with respect to a reverse of circular polarizations of both the incident and the scattered wave. We have calculated the relevant difference spectra taking into account the electron Coulomb interaction. We found that instead of screening out the interference, the Coulomb interaction enhances the CDE-SDE interference. From our analysis it follows that the charge-spin interference can be observed in the difference spectra measured under the backscattering geometry with equal circular polarizations of both incident and scattered photons. Exactly under such experimental conditions, a broad Raman band has been observed in the frequency range of single particle transitions.⁸ Consequently, we suggest that this band is a direct manifestation of the CDE-SDE interference, although further experiments will be helpful for a thorough understanding of these interference phenomena.

This work was supported by the Grant No. 12527 from the Royal Swedish Academy of Sciences under the program Research Cooperation between Sweden and the former Soviet Union.

¹S. Das Sarma *et al.* cond-mat/0002256 (unpublished).

²M.I. D'yakonov and V.I. Perel', *Fiz. Tverd. Tela* **13**, 3581 (1971) [*Sov. Phys. Solid State* **13**, 3023 (1972)]; *Zh. Éksp. Teor. Fiz.* **60**, 1954 (1971) [*Sov. Phys. JETP* **33**, 1053 (1971)].

³P. Ramvall, B. Kowalski, and P. Omling, *Phys. Rev. B* **55**, 7160 (1997).

⁴P.D. Dresselhaus, C.M.A. Papavassiliou, R.G. Wheeler, and R.N. Sacks, *Phys. Rev. Lett.* **68**, 106 (1992); T. Hassenkam *et al.*, *Phys. Rev. B* **55**, 9298 (1997).

⁵B. Jusserand, D. Richards, H. Peric, and B. Etienne, *Phys. Rev. Lett.* **69**, 848 (1992).

⁶B. Jusserand, D. Richards, H. Peric, and B. Etienne, *Surf. Sci.* **305**, 247 (1994).

⁷A.G. Mal'shukov, K.A. Chao, and M. Willander, *Phys. Rev. B* **55**, R1918 (1997).

⁸D. Richards and B. Jusserand, *Phys. Rev. B* **59**, R2506 (1999).

⁹V.A. Frol'tsov, A.G. Mal'shukov, and K.A. Chao, *Phys. Rev. B* **60**, 14 255 (1999).

¹⁰S. Das Sarma and D.-W. Wang, *Phys. Rev. Lett.* **83**, 816 (1999).

¹¹A. L. Fetter and J. D. Walecka, *Quantum Theory of Many-Particle Systems* (McGraw-Hill, New York, 1971).

¹²G. Dresselhaus, *Phys. Rev.* **100**, 580 (1955).

¹³Yu.A. Bychkov and E.I. Rashba, *J. Phys. C* **17**, 6039 (1984).

¹⁴A.A. Abrikosov and L.P. Gorkov, *Sov. Phys. JETP* **8**, 1090 (1959); S.F. Edwards, *Philos. Mag.* **3**, 1020 (1958).

¹⁵E. L. Ivchenko and G. E. Pikus, in *Superlattices and Other Heterostructures*, 2nd ed. (Springer, Berlin, 1997).

¹⁶E.O. Kane, *J. Phys. Chem. Solids* **1**, 249 (1957).

¹⁷A. Pinczuk and G. Abstreiter, in *Light Scattering in Solids V*, edited by M. Cardona and G. Güntherodt, Topics in Applied Physics No. 66 (Springer, Berlin, 1989).